2094 *Inorg. Chem.* **1987**, *26*, 2094-2101

Contribution from the Department of Chemistry,
State University of New York at Albany, Albany, New York 12222

Coordination Chemistry of the Rhenium–Organodiazenido Core with Facultative Tetradentate Ligands Possessing Thiolate–Amine and Thiolate–Thioether Donor Sets. Crystal and Molecular Structures of $[Re(SCH_2CH_2NMeCH_2CH_2NMeCH_2CH_2S)(N_2COC_6H_4\text{-}p\text{-}Cl)(PPh_3)]\cdot CH_3OH$, $[Re(SCH_2CH_2S(CH_2)_3SCH_2CH_2S)(N_2COPh)(PPh_3)]$, and $[Re(SCH_2CH_2S(CH_2)_3SCH_2CH_2S)(N_2CO_2Me)(PPh_3)]\cdot CH_2Cl_2$ and a Comparison with the Structure of the Oxidation Product [*N*,*N*′-Dimethyl-*N*,*N*′-bis(sulfinatoethyl)ethylenediamine-*S*,*N*,*N*′,*O*′][(2-chlorophenyl)diazenido](triphenylphosphine)rhenium(I), $[Re\{O_2SCH_2CH_2NMeCH_2CH_2NMeCH_2CH_2SO_2\}(N_2C_6H_4\text{-}o\text{-}Cl)(PPh_3)]$

Terrence Nicholson and Jon Zubieta*

Received October 10, 1986

The syntheses, crystal structures, electronic spectra, and electrochemical characteristics of a series of rhenium–organodiazenido complexes with facultative tetradentate ligands are reported. Complexes of the type $[Re\{SCH_2CH_2X(CH_2)_nXCH_2CH_2S\}(N_2R)(PPh_3)]$ ($X = NCH_3$, $n = 2$, $R = -COC_6H_4Cl$ (**1**); $X = S$, $n = 3$, $R = -COC_6H_5$ (**2**); $X = S$, $n = 3$, $R = -CO_2Me$ (**3**)) are synthesized from the reaction of $[ReCl_2(PPh_3)_2(N_2R)]$ complexes with the appropriate tetradentate ligand. Crystal data: for **1**, monoclinic space group $P2_1/n$, $a = 8.683$ (2) Å, $b = 18.278$ (4) Å, $c = 24.691$ (4) Å, $\beta = 97.95$ (1)°, $V = 3881.2$ (8) Å^3, $Z = 4$, $R = 0.055$ for 2469 reflections; for **2**, monoclinic space group $P2_1/n$, $a = 11.804$ (3) Å, $b = 12.529$ (3) Å, $c = 21.448$ (4) Å, $\beta = 89.39$ (1) Å, $V = 3171.8$ (9) Å^3, $Z = 4$, $R = 0.068$ for 2981 reflections; for **3**, monoclinic space group $P2_1/n$, $a = 8.570$ (2) Å, $b = 10.720$ (2) Å, $c = 35.618$ (6) Å, $\beta = 90.14$ (11)°, $V = 3272.3$ (11) Å^3, $Z = 4$, $R = 0.061$ for 3172 reflections. The structures display rhenium centers in distorted octahedral environments, with coordination sites occupied by two thiolate donors and two amine or sulfido donors from the tetradentate ligands, the phosphorus donor of the PPh_3 group, and the α-nitrogen of the linearly end-on coordinated organodiazenido group. The complexes are electrochemically active, exhibiting reversible 1-electron oxidations in the +0.3 to +0.5 V range. The more electron withdrawing the diazenido substituent R, the more positive the oxidation potential, suggesting that the oxidation potential is a measure of the energy of the HOMO. Although complexes of type **1**–**3** exhibit no tendency toward oxidation under ambient conditions, reaction of $[ReCl_2(PPh_3)_2(NH_3)(NNC_6H_4Cl)]$ with *N*,*N*′-dimethyl-*N*,*N*′-bis(mercaptoethyl)ethylenediamine yields a product, **4**, which oxidizes during subsequent chromatographic purification to yield the sulfinato derivative $[Re\{O_2SCH_2CH_2N(CH_3)CH_2CH_2N(CH_3)CH_2CH_2SO_2\}(N_2C_6H_4Cl)(PPh_3)]$ (**5**). Crystal data: for **5**, triclinic space group $P\bar{1}$, $a = 9.060$ (3) Å, $b = 10.499$ (3) Å, $c = 19.050$ (4) Å, $\alpha = 78.18$ (1)°, $\beta = 84.85$ (1)°, $\gamma = 76.34$ (1)°, $V = 1722.5$ (10) Å^3, $Z = 2$, $R = 0.077$ for 3395 reflections. The pseudooctahedral geometry about the rhenium center is generated by two amine donors, a sulfur from one sulfinato group and an oxygen from the second sulfinato group of the oxidized tetradentate ligand, the PPh_3 phosphorus donor, and the α-nitrogen of the organodiazenido ligand. The structure provides the first example of a complex exhibiting coordination through the oxygen of one sulfinate group and the sulfur of the second sulfinato moiety.

The current interest in metal–sulfur complexes derives from their potential relevance to active sites in metalloenzymes[1,2] and also from their essential role in heterogeneous catalysis.[3] Thus, the chemistry of molybdenum–thiolato and molybdenum-sulfido complexes is under intense scrutiny as representative of structural or functional models for biological or inorganic catalysts. In contrast, the chemistry of the elements of group VII (group 7[33]) with sulfur ligands remains relatively unexplored.[4,5]

A certain parallel between molybdenum and rhenium chemistry is suggested by the diagonal relationship, one that certainly appears to extend to the area of sulfur ligand chemistry where analogous structural types have been characterized such as $[MS_4]^{n-}$, $[MO(SPh)_4]^-$, and $[M_2O_3(\text{dithiocarbamate})_4]$.[6] More recently, we have sought to extend the analogies in molybdenum and rhenium chemistries to investigations of the relative abilities of the metal–thiolate cores to incorporate small organic molecules, such as CO, NO, and organohydrazines.[7,8] Complexes with organohydrazine ligands are particularly attractive in this respect as the varied structural frameworks and overall stability of the metal–organohydrazido cores provide useful probes for the properties of sulfur-ligated metal ions.[9]

In this paper, we describe the synthesis and characterization of the first examples of rhenium–thiolate complexes incorporating diazenido functionalities, –NNR. An unusual feature of the chemistry of these rhenium(I) derivatives, $[Re(SXXS)(N_2R)(PPh_3)]$, is the contrasting stability of the mercapto sulfurs toward air oxidation to sulfinato moieties, a process dependent primarily upon the identity of the organodiazenido substituent R. Fur-

---

(1) Stiefel, E. I. *Prog. Inorg. Chem.* **1977**, 22, 1. Spence, J. T. *Coord. Chem. Rev.* **1983**, *48*, 59.

(2) Hagan, K. S.; Watson, A. D.; Holm, R. H. *Inorg. Chem.* **1984**, *23*, 2984.

(3) Holm, R. H. *Chem. Soc. Rev.* **1981**, *10*, 455. Coucouvanis, D. *Acc. Chem. Res.* **1981**, *14*, 201.

(4) For recent work on technetium–thiolate chemistry, see: Brenner, D.; Davison, A.; Lister-James, J.; Jones, A. G. *Inorg. Chem.* **1984**, *23*, 3793.

(5) For some recent work on rhenium–thiolate chemistry, see: Dilworth, J. R.; Neaves, B. D.; Hutchinson, D. P.; Blower, P. J.; Dilworth, J. R.; Hutchinson, J. P.; Zubieta, J. *Transition Met. Chem.* (*Weinheim, Ger.*) **1982**, 7, 353.

(6) Rouschais, G. *Chem. Rev.* **1974**, *74*, 531.

(7) (a) Bishop, P. T.; Dilworth, J. R.; Hutchinson, J.; Zubieta, J. *Inorg. Chim. Acta* **1984**, *84*, L15. (b) Dahlstrom, P. L.; Dilworth, J. R.; Shulman, P.; Zubieta, J. *Inorg. Chem.* **1982**, *21*, 933. (c) Burt, A. J.; Dilworth, J. R.; Leigh, G. J.; Zubieta, J. *J. Chem. Soc., Dalton Trans.* **1982**, 2295. (d) Bishop, P. t.; Dilworth, J. R.; Hutchinson, J.; Zubieta, J. *J. Chem. Soc., Chem. Commun.* **1982**, 1052. Dilworth, J. R.; Hutchinson, J.; Zubieta, J. *J. Chem. Soc., Chem. Commun.* **1983**, 1034. (f) Hsieh, T.-C.; Gebreyes, K.; Zubieta, J. *J. Chem. Soc., Chem. Commun.* 1984, 1172. (g) Hsieh, T.-C.; Zubieta, J. *Inorg. Chim. Acta* **1985**, *99*, 647. Bishop, P. T.; Dilworth, J. R.; Zubieta, J. *J. Chem. Soc., Chem. Commun.* **1985**, 257. Blower, P. J.; Dilworth, J. R.; Hutchinson, J.; Nicholson, T.; Zubieta, J. *J. Chem. Soc., Dalton Trans.* **1985**, 2639.

(8) Blower, P. J.; Dilworth, J. R.; Hutchinson, J. P.; Zubieta, J. *Transition Met. Chem.* (*Weinheim, Ger.*) **1982**, 7, 354. Blower, P. J.; Dilworth, J. R.; Nicholson, T.; Zubieta, J. *Inorg. Chim. Acta* **1985**, *101*, 63. Nicholson, T.; Shaikh, N.; Zubieta, J. *Inorg. Chim. Acta* **1985**, *99*, L45. Blower, P. J.; Dilworth, J. R.; Hutchinson, P.; Zubieta, J. *J. Chem. Soc., Dalton Trans.*, **1985**, 1533.

(9) Dilworth, J. R.; Zubieta, J. *J. Chem.* Soc., *Chem. Commun.* **1981**, 132.

0020-1669/87/1326-2094$01.50/0

Scheme I

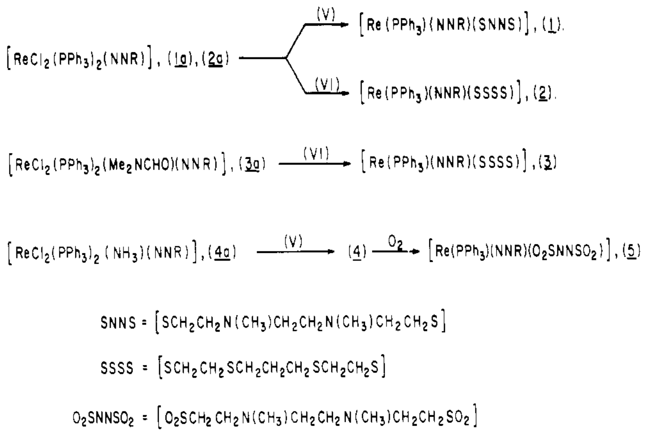

thermore, the organosulfinato ligand is ambidentate, capable of coordination through an oxygen (I) or sulfur (II) donor[10] or of coordination in a bidentate chelating mode (III).[11] Curiously, the structure of $[Re\{O_2SCH_2CH_2N(CH_3)CH_2CH_2N(CH_3)CH_2CH_2SO_2\}(N_2C_6H_4Cl\text{-}2)(PPh_3)]$ (**5**) described herein exhibits coordination through the oxygen of one arm and sulfur of the other (IV).

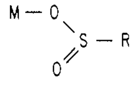

(I)

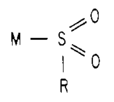

(II)

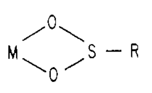

(III)

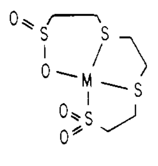

(IV)

Results and Discussion

Preparation and Spectroscopic Characterization of the Complexes. We have investigated the reactions of synthetic precursors containing rhenium–organohydrazido linkages with facultative tetradentate ligands with thiolate–amine or thiolate–thioether donors (V and VI).[12,13] The products fall into two categories depending on the nature of the substituent on the coordinated organodiazenido, –NNR, unit. Thus, for R = $-COPh$ or $-CO_2Me$, products of the general type $[Re(SNNS)(NNR)(PPh_3)]$ or $[Re(SSSS)(NNR)(PPh_3)]$ are isolated, whereas for R = $-C_6H_4X$, facile air oxidation occurs at the coordinated mercapto sulfur atoms to yield bis(sulfinato) derivatives, $[Re(O_2SNNSO_2)(NNR)(PPh_3)]$, as shown in the Scheme I.

Reactions of the six coordinate organohydrazido(3–) chelate (O,N) complexes $[ReCl_2(PPh_3)_2(NNR)$, R = $-COPh$[14] or $-COC_6H_4Cl$, are known to occur via chelate ring opening and displacement of the carbonyl oxygen by a donor group of the incoming ligand. Thus, the reactions of benzoylhydrazido "green chelate", $[ReCl_2(PPh_3)_2(NNCOPh)]$, and the (chlorobenzoyl)hydrazido derivative $[ReCl_2(PPh_3)_2(N_2COC_6H_4\text{-}o\text{-}Cl)]$ with the tetradentate ligands V and VI yield diamagnetic complexes $[Re(NNCOPh)(PPh_3)(SXXS)]$, X = S (**2**), and $[Re(N_2COC_6H_4\text{-}o\text{-}Cl)(PPh_3)(SXXS)]$, X = NCH_3 (**1**). The (carboxymethyl)hydrazido(3–) complex $[ReCl_2(PPh_3)_2(Me_2NCHO)(NNCO_2Me)]$ reacts in an analogous fashion, with displacement of the weakly coordinated dimethylformamide to yield $[Re(NNCO_2Me)(PPh_3)(SSSS)]$ (**3**). As formulated, the complexes are described as containing the (organodiazenido)rhenium(I) core, $[Re{=}N{=}N{-}R]^{2+}$, a formalism consistent with the observed diamagnetism and the infrared and electronic spectra of the complexes. The infrared spectra of the chelate precursors $[ReCl_2(PPh_3)_2(NNR)]$, R = $-COPh$ and $-COC_6H_4Cl$, exhibit no bands assignable to $\nu(C{=}O)$ or $\nu(N{=}N)$ whereas $[ReCl_2(PPh_3)_2(Me_2NCHO)(NNCOOMe)]$ shows a single band at 1740 cm^{-1} in the IR spectrum, suggesting coordination through the amide nitrogen rather than the carbonyl oxygen of dimethylformamide.[15] Products **1**–**3** show characteristic bands in the 1500–1650-cm^{-1} region, assigned to $\nu(N{=}N)$ and $\nu(C{=}O)$ of the organodiazenido functionality. The electronic spectra of the products present intense charge transfer bands in the 300–420-nm region. The transition observed at ca. 400–415 nm for all complexes appears to be characteristic of the $[ReNNR]^{2+}$ chromophore. The low-wavelength charge-transfer band displays a hypsochromic shift from 345 nm in the spectrum of **1** to ca. 320 nm in the spectra of **2** and **3** upon substitution of thioether groups for amine donors. The spectrum of **2** exhibits an additional band at 360 nm, presumably associated with S(thioether) $\rightarrow$ Re charge transfer.

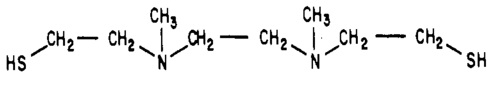

(V), HSNNSH

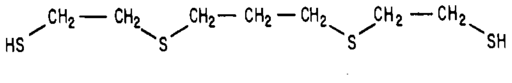

(VI), HSSSSH

In order to investigate the influence of the organohydrazido substituents on the chemistry, we prepared $[ReCl_2(N_2C_6H_4X)(NH_3)(PPh_3)_2]$ by the reaction of $[ReOCl_3(PPh_3)_2]$ with $H_2NNHC_6H_4X{\cdot}HCl$.[16] Reaction of $[ReCl_2(N_2C_6H_4Cl)(NH_3)(PPh_3)_2]$ with V in benzene under an N_2 atmosphere yields a brown residue analyzing as $[Re(NNC_6H_4Cl)(PPh_3)(SNNS)]$ (**4**) and spectroscopically similar to species **1**–**3**. Upon exposure to O_2, solutions of the complex turned red-orange and upon purification by silica chromatography yielded bright cherry red crystals of **5**. The infrared spectrum of this material exhibited strong bands in the 1200–1220- and 1030–1075-cm^{-1} regions, which are attributed to $\nu_a(SO_2)$ and $\nu_s(SO_2)$.[17] The X-ray structural studies confirmed the presence of the sulfinato units (vide infra). Treatment of the material (**4**) with *m*-chloroperbenzoic acid or with hydrogen peroxide[18] yielded only insoluble materials and polymeric organosulfides. Oxidation of **4** to the sulfinato derivative **5** is most readily effected by passing an ox-

---

(10) Lundeen, M.; Firor, R. L.; Seff, K. *Inorg. Chem.* **1978**, *17*, 701. Elder, R. C.; Heeg, M. J.; Payne, M. D.; Trkula, M.; Deutsch, E. *Inorg. Chem.* **1978**, *17*, 431. Higashi, L. S.; Lundeen, M.; Hilti, E.; Seff, K. *Inorg. Chem.* **1977**, *16*, 310. Lange, B. A.; Libson, K.; Deutsch, E.; Elder, R. C. *Inorg. Chem.* **1976**, *15*, 2985. Sloan, C. P.; Krueger, J. H. *Inorg. Chem.* **1975**, *14*, 1481.

(11) Bertz, S. H.; Dabbagh, G. *Inorg. Chem.* **1985**, *24*, 3488. Kubota, M.; Rothrock, R. K.; Kernan, M. R.; Hauen, R. B. *Inorg. Chem.* **1982**, *21*, 2491.

(12) Rosen, W.; Busch, D. H. *J. Am. Chem. Soc.* **1969**, *91*, 4694.

(13) Karlin, K. D.; Lippard, S. J. *J. Am. Chem. Soc.* **1976**, *98*, 6951.

(14) Chatt, J.; Dilworth, J. R.; Leigh, P. J.; Gupta, V. *J. Chem. Soc. A* **1971**, 2631.

(15) Nicholson, T.; Zubieta, J., submitted for publication in *Inorg. Chem.*

(16) Dilworth, J. R.; Harrison, S. A.; Walton, D. R. M.; Schweda, E. *Inorg. Chem.* **1985**, *24*, 2594.

(17) Vitzthum, G.; Lindner, E. *Angew. Chem., Int. Ed. Engl.* **1971**, *10*, 315.

(18) Schubert, M. P. *J. Am. Chem. Soc.* **1933**, *55*, 3336.

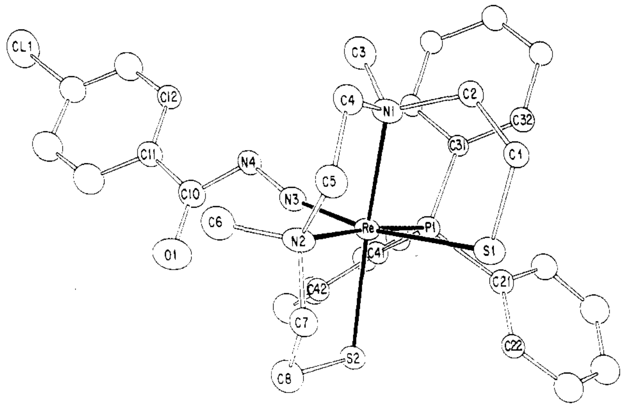

Figure 1. ORTEP view of the structure of **1**, showing 50% probability ellipsoids.

Table I. Atom Coordinates (×10⁴) and Temperature Factors (Å² × 10³) for **1**

atom	x	y	z	U_{iso}[a]
Re	890 (1)	299 (1)	1866 (1)	36 (1)
P(1)	498 (5)	−352 (3)	2684 (2)	38 (2)
S(1)	1308 (6)	1420 (3)	2418 (2)	51 (2)
S(2)	−1736 (6)	643 (3)	1680 (2)	54 (2)
Cl(1)	1955 (9)	5519 (3)	239 (3)	96 (3)
N(1)	3529 (16)	424 (8)	1919 (6)	46 (6)
N(2)	1077 (16)	922 (9)	1085 (7)	50 (6)
N(3)	927 (16)	−559 (8)	1544 (6)	45 (6)
N(4)	1303 (19)	−1211 (8)	1386 (7)	52 (6)
O(1)	−872 (18)	−1170 (8)	744 (7)	89 (7)
C(1)	3404 (22)	1525 (11)	2515 (9)	60 (6)
C(2)	4235 (24)	850 (11)	2416 (8)	60 (6)
C(3)	4392 (25)	−270 (11)	1935 (9)	66 (6)
C(4)	3910 (23)	831 (12)	1442 (8)	59 (6)
C(5)	2552 (27)	1320 (14)	1164 (11)	88 (8)
C(6)	1032 (28)	446 (12)	627 (9)	79 (7)
C(7)	−252 (26)	1396 (13)	987 (10)	75 (7)
C(8)	−1737 (26)	1036 (13)	1009 (9)	72 (7)
C(10)	320 (26)	−1508 (11)	995 (9)	54 (6)
C(11)	742 (22)	−2257 (10)	840 (8)	50 (5)
C(12)	1931 (20)	−2635 (10)	1102 (8)	45 (5)
C(13)	2262 (25)	−3338 (12)	920 (9)	65 (6)
C(14)	1466 (24)	−3601 (12)	494 (9)	57 (6)
C(15)	206 (25)	−3258 (12)	199 (10)	70 (7)
C(16)	−139 (27)	−2605 (13)	406 (9)	75 (7)
C(21)	−426 (21)	109 (10)	3209 (7)	45 (5)
C(22)	−1486 (20)	693 (10)	3085 (7)	41 (5)
C(23)	−2223 (24)	1008 (12)	3491 (8)	62 (6)
C(24)	−2070 (24)	746 (12)	3985 (9)	68 (6)
C(25)	−1064 (26)	172 (13)	4138 (10)	75 (7)
C(26)	−239 (24)	−143 (11)	3741 (8)	56 (6)
C(31)	2258 (18)	−723 (9)	3071 (7)	33 (4)
C(32)	3183 (23)	−315 (11)	3464 (8)	58 (6)
C(33)	4642 (25)	−571 (11)	3702 (9)	65 (6)
C(34)	5125 (30)	−1238 (13)	3545 (10)	82 (8)
C(35)	4220 (26)	−1657 (14)	3146 (9)	78 (7)
C(36)	2774 (23)	−1399 (11)	2892 (8)	57 (6)
C(41)	−751 (22)	−1166 (10)	2564 (8)	50 (5)
C(42)	−1757 (22)	−1243 (11)	2062 (8)	55 (6)
C(43)	−2763 (28)	−1860 (13)	2006 (10)	80 (7)
C(44)	−2695 (25)	−2347 (13)	2427 (9)	71 (7)
C(45)	−1763 (22)	−2272 (11)	2892 (8)	54 (6)
C(46)	−765 (22)	−1703 (11)	2982 (8)	53 (6)
O(2)	4754 (36)	1962 (17)	111 (13)	83 (9)
C(sol)	5083 (71)	8762 (34)	363 (24)	126 (22)
H(sa)	4007	8873	374	252
H(sb)	5611	9194	267	252
H(sc)	5550	8592	716	252

[a] Equivalent isotropic U defined as one-third of the trace of the orthogonalized $\mathbf{U}_{\text{iso}}$ tensor.

ygenated solution through a silica column. Since all attempts to oxidize the coordinated mercapto- ligands of complexes **1–3** proved unsuccessful, we conclude that this chemistry is unique to the (aryldiazenido)rhenium complexes of type **4**, suggesting a structure

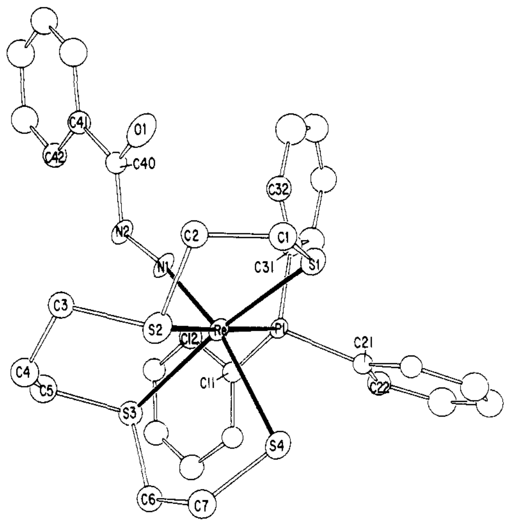

Figure 2. ORTEP representation of the structure of **2**, showing 50% probability ellipsoids.

Table II. Atom Coordinates (×10⁴) and Temperature Factors (Å² × 10³) for **2**

atom	x	y	z	U_{iso}[a]
Re	3297 (1)	7001 (1)	3496 (1)	31 (1)
P	2403 (3)	m159 (3)	4510 (2)	30 (1)
S(1)	1742 (4)	6048 (4)	3103 (2)	44 (1)
S(2)	4099 (4)	6754 (4)	2457 (2)	53 (2)
S(3)	5139 (4)	7722 (4)	3853 (2)	42 (1)
S(4)	4217 (4)	5312 (3)	3794 (3)	53 (2)
N(1)	2951 (11)	8361 (9)	3363 (6)	32 (4)
N(2)	2851 (11)	9368 (10)	3365 (6)	35 (4)
O	1598 (12)	9206 (9)	2525 (6)	62 (5)
C(11)	3317 (13)	7874 (12)	5045 (7)	36 (4)
C(12)	3196 (14)	8998 (14)	5100 (8)	48 (4)
C(13)	3987 (14)	9550 (15)	5446 (8)	48 (5)
C(14)	4874 (15)	9031 (16)	5728 (9)	55 (5)
C(15)	5011 (17)	7975 (14)	5654 (9)	56 (5)
C(16)	4212 (13)	7385 (14)	5318 (7)	40 (4)
C(21)	1976 (12)	5981 (12)	4971 (7)	33 (4)
C(22)	1869 (14)	6067 (15)	5624 (8)	47 (4)
C(23)	1424 (17)	5193 (17)	5960 (11)	71 (6)
C(24)	1127 (16)	4277 (16)	5645 (9)	59 (5)
C(25)	1280 (15)	4226 (17)	5026 (9)	60 (5)
C(26)	1695 (12)	5031 (13)	4670 (8)	38 (4)
C(31)	1060 (14)	7903 (13)	4484 (8)	39 (4)
C(32)	577 (15)	8167 (14)	3932 (9)	48 (5)
C(33)	−444 (18)	8689 (18)	3941 (11)	77 (7)
C(34)	−1006 (18)	8952 (18)	4486 (10)	68 (6)
C(35)	−561 (16)	8746 (16)	5019 (10)	62 (6)
C(36)	523 (17)	8234 (16)	5062 (10)	59 (5)
C(40)	2081 (12)	9748 (12)	2944 (7)	34 (4)
C(41)	1792 (13)	10912 (14)	3015 (8)	40 (4)
C(42)	2312 (15)	11526 (15)	3470 (8)	48 (5)
C(43)	2028 (17)	12598 (17)	3528 (10)	64 (6)
C(44)	1193 (17)	13050 (17)	3169 (10)	66 (6)
C(45)	691 (16)	12424 (17)	2735 (10)	59 (5)
C(46)	979 (16)	11386 (16)	2646 (10)	60 (5)
C(1)	2033 (16)	5844 (16)	2263 (9)	60 (5)
C(2)	2791 (18)	6714 (17)	2004 (11)	68 (6)
C(3)	4684 (19)	8019 (17)	2239 (11)	74 (6)
C(4)	5775 (23)	8210 (22)	2576 (13)	97 (8)
C(5)	5734 (21)	8542 (20)	3224 (11)	87 (7)
C(6)	6051 (21)	6622 (19)	3942 (12)	88 (7)
C(7)	5659 (20)	5580 (21)	3635 (13)	96 (8)

[a] Equivalent isotropic U defined as one-third of the trace of the orthogonalized $\mathbf{U}_{\text{iso}}$ tensor.

distinct in detail from that observed for **1–3**. We have been unsuccessful in our attempts to crystallize species of class **4** and to confirm this structural speculation.

Description of the Structures. The structures of the complexes of the general class [Re{S(CH$_2$)$_2$X(CH$_2$)$_n$X(CH$_2$)$_2$S}(NNR)(PPh$_3$)] are illustrated in Figures 1–3, for **1** (X = −NMe, n =

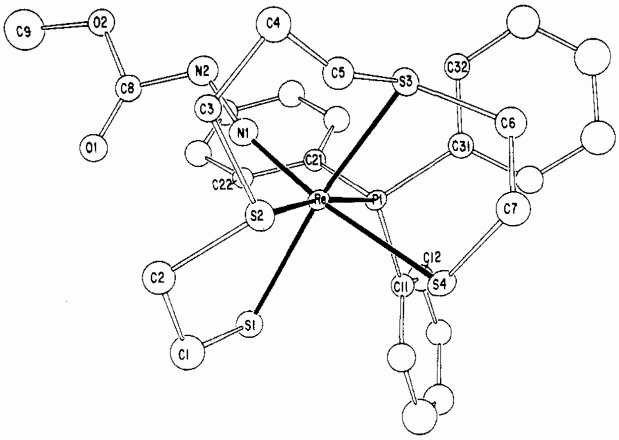

Figure 3. ORTEP view of the structure of **3**, showing 50% probability ellipsoids.

Table III. Atom Coordinates ($\times 10^4$) and Temperature Factors ($Å^2 \times 10^3$) for **3**

atom	x	y	z	$U_{iso}{}^a$
Re	1049 (1)	1919 (1)	832 (1)	25 (1)
P(1)	1859 (4)	1788 (4)	1481 (1)	28 (1)
S(1)	3363 (5)	941 (4)	612 (1)	37 (1)
S(2)	235 (5)	1788 (4)	184 (1)	38 (1)
S(3)	−1620 (5)	2567 (4)	991 (1)	37 (1)
S(4)	−91 (5)	−182 (4)	917 (1)	41 (1)
N(1)	1634 (13)	3501 (10)	809 (3)	26 (4)
N(2)	1758 (15)	4711 (13)	825 (4)	45 (5)
O(1)	3992 (15)	4647 (11)	482 (4)	62 (5)
O(2)	3059 (15)	6417 (11)	742 (4)	62 (5)
Cl(1)	8411 (12)	6543 (10)	1204 (5)	106 (7)
Cl(2)	10218 (22)	6855 (13)	1909 (4)	137 (8)
C(sol)	10234 (36)	6840 (30)	1432 (8)	37 (7)
C(1)	3103 (21)	873 (18)	105 (5)	54 (5)
C(2)	2107 (20)	1850 (17)	−55 (5)	49 (4)
C(3)	−544 (23)	3270 (18)	41 (6)	64 (6)
C(4)	−1815 (25)	3791 (21)	309 (6)	72 (6)
C(5)	−2692 (23)	2917 (19)	557 (5)	61 (5)
C(6)	−2652 (19)	1201 (16)	1134 (5)	46 (4)
C(7)	−2206 (21)	88 (18)	933 (5)	53 (5)
C(8)	3044 (19)	5183 (16)	661 (4)	41 (4)
C(9)	4419 (28)	7118 (23)	595 (7)	91 (8)
C(11)	3024 (17)	468 (15)	1668 (4)	35 (4)
C(12)	3595 (19)	542 (17)	2027 (5)	47 (4)
C(13)	4452 (20)	−409 (17)	2181 (5)	52 (5)
C(14)	4804 (24)	−1448 (21)	1969 (5)	67 (6)
C(15)	4260 (25)	−1551 (22)	1592 (6)	75 (6)
C(16)	3361 (20)	−585 (17)	1447 (5)	50 (5)
C(21)	3080 (17)	3106 (15)	1621 (4)	32 (3)
C(22)	4206 (17)	3495 (14)	1373 (4)	32 (4)
C(23)	5210 (20)	4462 (17)	1453 (5)	49 (5)
C(24)	5065 (22)	5067 (19)	1792 (5)	57 (5)
C(25)	3982 (20)	4734 (18)	2053 (5)	54 (5)
C(26)	3002 (20)	3706 (18)	1961 (5)	49 (5)
C(31)	247 (18)	1821 (15)	1809 (4)	39 (4)
C(32)	−590 (19)	2921 (16)	1852 (4)	41 (4)
C(33)	−1924 (24)	2950 (20)	2080 (6)	67 (6)
C(34)	−2406 (28)	1887 (21)	2260 (6)	81 (7)
C(35)	−1616 (24)	737 (22)	2209 (6)	71 (6)
C(36)	−241 (20)	758 (17)	1985 (4)	46 (4)

[a] Equivalent isotropic U defined as one-third of the trace of the orthogonalized $\mathbf{U}_{iso}$ tensor.

2, R = $-N_2COC_6H_4Cl$), **2** (X = S, n = 3, R = $-N_2COC_6H_5$), and **3** (X = S, n = 3, R = $-N_2CO_2Me$), respectively. Atomic coordinates are listed in Tables I–III, and selected structural parameters are given in Tables V and VI.

The structure of **1** provides a prototype for the geometries of this class. Complex **1** crystallizes as discrete monomers, with the rhenium atom in a distorted octahedral environment. The coordination sites are occupied by the two amine nitrogen donors and the two thiolate donors of the tetradentate ligand, the phosphorus donor of the PPh_3 group, and the α-nitrogen of the (chlorobenzoyl)diazenido unit. The thiolate donors exhibit an unusual cis orientation, while the amino ligands are constrained to adopt the mutually cis orientation by virtue of their location as internal donors of the linear tetradentate ligand. Linear tetradentate ligands with terminal thiolate functionalities exhibit the

Table IV. Atom Coordinates ($\times 10^4$) and Temperature Factors ($Å^2 \times 10^3$) for **5**

atom	x	y	z	$U_{iso}{}^a$
Re	2820 (1)	1536 (1)	3161 (1)	27 (1)
S(1)	5156 (7)	173 (5)	3634 (3)	35 (2)
S(2)	1641 (10)	3282 (7)	4502 (4)	60 (3)
P(1)	3836 (7)	3440 (5)	2530 (3)	30 (2)
Cl(1)	1428 (11)	434 (11)	442 (4)	94 (4)
O(5)	1107 (25)	2379 (20)	6580 (11)	73 (6)
N(1)	2988 (21)	980 (17)	2346 (9)	34 (4)
N(2)	2575 (26)	742 (21)	1758 (11)	54 (5)
N(3)	1929 (24)	−228 (19)	3797 (10)	43 (5)
N(4)	323 (22)	2356 (17)	3093 (9)	36 (4)
O(1)	2413 (18)	2132 (14)	4136 (7)	36 (3)
O(2)	605 (32)	2719 (25)	5105 (14)	83 (7)
O(3)	6072 (20)	−614 (15)	3134 (8)	48 (4)
O(4)	6051 (19)	771 (15)	4012 (8)	42 (4)
C(1)	4492 (26)	−1110 (21)	4329 (11)	37 (5)
C(2)	2791 (27)	−739 (23)	4452 (12)	40 (5)
C(3)	2180 (34)	−1370 (26)	3363 (14)	57 (7)
C(4)	293 (29)	216 (24)	3944 (13)	48 (6)
C(5)	−389 (34)	1117 (26)	3294 (14)	59 (7)
C(6)	−320 (30)	3110 (23)	2396 (12)	45 (6)
C(7)	−645 (41)	3263 (33)	3637 (18)	84 (10)
C(8)	376 (38)	4134 (30)	3842 (17)	74 (9)
C(11)	3558 (25)	−147 (19)	1413 (10)	29 (5)
C(12)	3227 (32)	−427 (25)	769 (13)	52 (6)
C(13)	4144 (34)	−1304 (27)	380 (15)	61 (7)
C(14)	5618 (37)	−2071 (30)	653 (16)	68 (8)
C(15)	6032 (34)	−1833 (26)	1287 (14)	55 (7)
C(16)	4942 (33)	−877 (26)	1642 (14)	56 (7)
C(21)	5420 (27)	3072 (21)	1839 (11)	36 (5)
C(22)	6298 (28)	1890 (23)	1874 (12)	42 (6)
C(23)	7496 (36)	1661 (29)	1383 (15)	63 (7)
C(24)	7784 (35)	2635 (27)	834 (15)	62 (7)
C(25)	6851 (34)	3881 (28)	777 (15)	61 (7)
C(26)	5607 (30)	4126 (24)	1253 (12)	46 (6)
C(31)	4728 (24)	4305 (19)	3062 (10)	28 (4)
C(32)	5002 (27)	3798 (22)	3779 (11)	38 (5)
C(33)	5737 (28)	4441 (22)	4179 (12)	43 (6)
C(34)	6142 (32)	5591 (24)	3876 (13)	49 (6)
C(35)	5824 (33)	6147 (27)	3159 (14)	57 (7)
C(36)	5099 (32)	5536 (25)	2769 (14)	54 (7)
C(41)	2494 (30)	4802 (23)	1966 (12)	45 (6)
C(42)	2123 (34)	4512 (27)	1365 (14)	59 (7)
C(43)	921 (41)	5535 (32)	954 (18)	80 (9)
C(44)	217 (49)	6668 (39)	1160 (21)	102 (12)
C(45)	579 (43)	6982 (37)	1776 (18)	89 (10)
C(46)	1776 (34)	5972 (26)	2210 (15)	59 (7)

[a] Equivalent isotropic U defined as one-third of the trace of the orthogonalized $\mathbf{U}_{iso}$ tensor.

Table V. Selected Bond Lengths (Å), Angles (deg), and Contact Distances (Å) for $[Re(SCH_2CH_2NMeCH_2CH_2NMeCH_2CH_2S)(NNOCOC_6H_4\text{-}p\text{-}Cl)(PPh_3)]$ (**1**)

Re–P	2.409 (5)	P–Re–S(1)	88.5 (2)
Re–S(1)	2.459 (5)	P–Re–S(2)	92.9 (2)
Re–S(2)	2.348 (5)	P–Re–N1)	104.9 (4)
Re–N(1)	2.29 (1)	P–Re–N(2)	176.0 (4)
Re–N(2)	2.27 (1)	P–Re–N(3)	87.2 (5)
Re–N(3)	1.76 (2)	S(1)–Re–S(2)	87.2 (2)
N(3)–N(4)	1.31 (2)	S(1)–Re–N(2)	79.4 (4)
N(4)–C(10)	1.31 (2)	S(1)–Re–N(2)	91.8 (4)
C(10)–O	1.29 (3)	S(1)–Re–N(3)	169.0 (5)
S1···N1	3.034	S(2)Re–N1)	157.2 (4)
S2···N2	3.063	S(2)–Re–N(2)	83.2 (4)
N1···N2	2.898	S(2)–Re–N3)	103.2 (5)
		N(1)Re–N(2)	79.0 (5)
		N(1)–Re–N(3)	91.9 (6)
		N(2)–Re–N(3)	93.2 (6)
		Re–N(3)–N(4)	165.1 (12)

Table VI. Selected Bond Lengths (Å), Angles (deg), and Contact Distances (Å) for [Re($SCH_2CH_2SCH_2CH_2CH_2SCH_2CH_2S$)($NNCOC_6H_5$)($PPh_3$)] (**2**) and [Re($SCH_2CH_2SCH_2CH_2CH_2SCH_2CH_2S$)($NNCO_2Me$)($PPh_3$)] (**3**)

	2	3
Re-P	2.414 (4)	2.406 (4)
Re-S(1)	2.354 (4)	2.377 (4)
Re-S(2)	2.432 (5)	2.404 (4)
Re-S(3)	2.483 (5)	2.458 (4)
Re-S(4)	2.466 (5)	2.473 (4)
Re-N(1)	1.776 (12)	1.770 (11)
N(1)-N(2)	1.27 (2)	1.30 (2)
N(2)-C(40)	1.37 (2)	1.35 (2)
C(40)-O	1.27 (2)	1.18 (2)
S(1)···S(2)	3.213	3.212
S(2)···S(3)	3.528	3.237
S(3)···S(4)	3.213	3.237
P-Re-S(1)	91.7 (1)	92.9 (1)
P-Re-S(2)	176.1 (2)	173.3 (1)
P-Re-S(3)	93.9 (1)	93.5 (1)
P-Re-S(4)	91.5 (2)	86.7 (1)
P-Re-N(1)	88.1 (4)	90.0 (4)
S(1)-Re-S(2)	84.5 (2)	84.2 (1)
S(1)-Re(S(3)	169.7 (1)	168.0 (1)
S(1)-Re-S(4)	90.3 (2)	88.2 (1)
S(1)-Re-N(1)	104.3 (4)	99.8 (4)
S(2)-Re-S(3)	89.7 (2)	88.3 (1)
S(2)-Re-S(4)	87.7 (2)	87.2 (1)
S(2)-Re-N(1)	93.6 (4)	95.3 (4)
S(3)-Re-S(4)	80.9 (2)	82.0 (1)
S(3)-Re-N(1)	84.5 (4)	90.2 (4)
S(4)-Re-N(1)	165.4 (4)	171.8 (4)
Re-N(1)-N(2)	167.5 (12)	167.0 (10)

trans thiolate configuration in all other instances of octahedrally coordinated metal complexes studied to date.[19] In fact, the trans thiolate arrangement is characteristic of most pseudooctahedral structures of the general classes [$ML_2(SXXS)$], [$ML_2(SX)_2$], and [$ML_4(SR)_2$] (where X represents a nitrogen donor, SXXS a tetradentate ligand of the linear or tripodal types, and SX a bidentate ligand), with the exception of certain rare instances where severe steric constraints impose pseudocis thiolate geometry.[20] The more common disposition of donor groups for linear tetradentate ligands in complexes with the metal–diazenido core is illustrated by the structure of [Mo($N_2C_6H_4OMe$)$_2$($SCH_2CH_2NMeCH_2CH_2NMeCH_2CH_2S$)], where the thiolate donors occupy mutually trans positions with the amine donors oriented trans to the diazendo units.[7b] A consequence of the cis thiolate geometry is to dispose the thiolate donor S(1) trans to the diazenido unit. This orientation is most unusual as thiolate donors are generally disposed cis to strongly π-bonding groups, such as oxo or diazenido functionalities, although recent structural studies reveal that diazenido groups permit greater structural flexibility than that allowed by the oxo donor.[7]

The strong trans influence of the diazenido group is evident in the Re–S(1) distance of 2.459 (5) Å compared to a distance of 2.348 (5) Å for Re–S(2), which falls into the range of 2.32–2.37 Å generally observed for Re–thiolate interactions. In contrast, the diazenido ligand exerts a minimal trans influence on trans chloride ligands,[21] an observation consistent with transmission of the effect through the ligand–metal–ligand π-system. This most likely reflects the significant thiolate-to-metal π-donor interaction.

The Re–NNR unit displays metrical parameters consistent with the metal–diazenido formalism. The short Re–N(3) and N(3)–N(4) distances, 1.76 (2) and 1.31 (2) Å, suggest extensive delocalization and multiple bonding throughout the unit, an observation confirmed by the virtual planarity of the entire Re–N–NCOC$_6$H$_4$Cl grouping and the linearity of the Re–N(3)–N(4) unit. Since the diazenido ligand functions formally as a three-electron donor (NNR)$^+$, the complex obeys the "18-electron rule" and is best described as a rhenium(I) species.

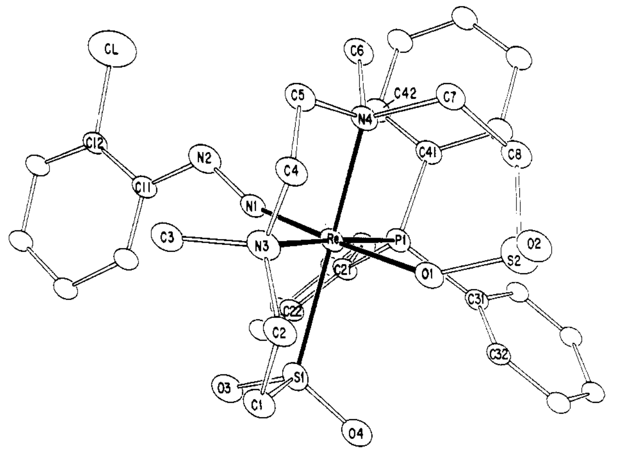

Figure 4. ORTEP representation of the structure of the sulfinato derivative **5**, showing 50% probability ellipsoids.

As a result of forming three five-membered chelate rings with the metal, the ligand chain is tightly wrapped; this produces significant deviations of the Re valence angles from those anticipated for regular octahedral geometry. The internal chelate angles are thus 79.4 (4), 79.0 (5), and 83.2 (4)° for S(1)–Re–N(1), N(1)–Re–N(2), and S(2)–Re–N(2), respectively. The chelate rings display unexceptional geometries.[7b,22] Atoms C(1) and C(2) are on opposite sides of the S(1)–Re–N(1) plane, and atoms C(5) and C(6) are on opposite sides of the S(2)–Re–N(1) plane, producing a symmetric skew conformation for the two C–N–Re–S–C rings.[23] The two methyl groups are on the same side of the diamine chelate ring.

The consequence of substituting sulfide donors for amine donors of the tetradentate ligand are illustrated by the structure of **2**, Figure 2. The overall geometry is similar to that observed for **1** with the rhenium in the pseudooctahedral environment generated by coordination to two thiolate and two sulfido donors from the tetradentate ligand, to the phosphorous of the PPh$_3$ group, and to the α-nitrogen of the benzoyldiazenido group. The thiolate donors are again disposed mutually cis, with S(4) occupying a position trans to the strongly π-bonding benzoyldiazenido ligand. The considerable trans influence exerted by the diazenido ligand is evident to the long Re–S(4) distance of 2.466 (5) Å, as compared to a value of 2.354 (4) Å observed for Re–S(1). The Re–S(4) distance is considerably longer than the 2.32–2.37 Å distance expected for a rhenium–thiolate interaction and is on the order of the Re–thioether distances Re–S(2) and Re–S(3), which are unexceptional for this type of interaction. The geometry of the metal–diazenido linkage is similar to that observed for **1**.

A further consequence of the three methylene bridge units and thioether donors rather than the two methylene bridges and amine donors, as in **1**, is to open the central, S(2)···S(3), ligand bite distance to 3.52 Å from the value of 2.90 Å observed for N(1)···N(2) in **1**.

The terminal arms of the tetradentate ligand exhibit the usual geometries. Thus, the rings C–S(1)–Re–S(2)–C and C–S(3)–Re–S(4)–C adopt the symmetric skew conformation. The six-membered ring C–C–S(2)–Re–S(3)–C adopts the symmetric chair conformation.

Substitution of a carboxylmethyl substituent for the benzoyl group of the organodiazenido ligand effects no significant changes in either the chemistry or the structures of these classes of complexes. Thus, the structure of **3**, shown in Figure 3, exhibits no characteristics significantly different from those discussed for **2**.

---

(19) Bruce, A.; Corbin, J. L.; Dahlstrom, P. L.; Hyde, J. R.; Minelli, M.; Stiefel, E. I.; Spence, J. T.; Zubieta, J. *Inorg. Chem.* **1982**, *21*, 917.

(20) Stiefel, E. I.; Miller, K. F.; Bruce, A. G.; Corbin, J. C.; Berg, J. M.; Hodgson, K. D. *J. Am. Chem. Soc.* **1980**, *102*, 3624.

(21) Nicholson, T.; Zubieta, J., submitted for publication in *Inorg. Chem.*

(22) Baltusis, L. M.; Karlin, K. D.; Rabinowitz, H. N.; Dewan, J. C.f Lippard, S. J. *Inorg. Chem.* **1980**, *19*, 2627. Hu, W.-J.; Lippard, S. J. *J. Am. Chem. Soc.* **1974**, *96*, 2366.

(23) Hawkin, C. J. *Absolute Configuration of Metal Complexes*; Wiley-Interscience: New York, 1971.

Table VII. Selected Bond Lengths (Å) and Angles (deg) for $[Re(O_2SCH_2CH_2NMeCH_2CH_2NMeCH_2CH_2SO_2)(NNC_6H_4Cl\text{-}2)(PPh_3)]$ (**5**)

Re–P	2.444 (6)	N(1)–N(2)	1.30 (2)
Re–S(1)	2.392 (6)	N(2)–C(11)	1.36 (3)
Re–N(3)	2.27 (2)	S(1)–O(3)	1.46 (2)
Re–N(4)	2.23 (2)	S(1)–O(4)	1.45 (2)
Re–N(1)	1.75 (2)	S(2)–O(1)	1.51 (2)
Re–O(1)	2.06 (2)	S(2)–O(2)	1.53 (3)
P–Re–S(1)	97.3 (2)	N(4)–Re–N(1)	93.7 (8)
P–Re–N(3)	81.0 (5)	N(4)–Re–O(1)	81.7 (6)
P–Re–N(4)	158.3 (4)	N(1)–Re–O(1)	174.2 (8)
P–Re–N(1)	97.2 (6)	Re–N(1)–N(2)	158.8 (17)
P–Re–O(1)	86.1 (4)	Re–O(1)–S(2)	143.7 (8)
S(1)–Re–N(3)	177.1 (5)	O(1)–S(2)–O(2)	106.1 (12)
S(1)–Re–N(4)	101.8 (5)	O(1)–S(2)–C(8)	97.8 (13)
S(1)–Re–N(1)	88.0 (6)	O(2)–S(2)–C(8)	102.8 (15)
S(1)–Re–O(1)	96.4 (5)	Re–S(1)–O(3)	113.6 (7)
N(3)–Re–N(4)	79.5 (7)	O(3)–S(1)–O(4)	117.7 (6)
N(3)–Re–N(1)	94.5 (8)	O(3)–S(1)–O(4)	113.0 (11)
N(3)–Re–O(1)	81.3 (7)		

The bond parameters for **2** and **3** are similar, as shown in Table VI, as are the overall geometries, shown in Figures 2 and 3. The folding pattern of the tetradentate ligand differs in that the central six-membered ring C–C–S(2)–Re–S(3)–C adopts a skew conformation rather than the symmetric chair presented by **2**.

The sulfinato derivative **5** exhibits the pseudooctahedral geometry depicted in Figure 4, with atomic coordinates listed in Table IV and bonding parameters given in Table VII. The oxidized tetradentate ligand provides two amine nitrogen donors, a sulfur from one sulfinato group, and an oxygen donor from the second sulfinato group, while the phosphorus of the PPh_3 and the α-nitrogen of the (chlorophenyl)diazenido group complete the coordination geometry. One amine nitrogen N(3) is trans to the PPh_3 group, while N(4) occupies a site trans to the sulfur-bonded sulfinato group, leaving the oxygen-bonded sulfinato group trans to the diazenido ligand. The Re–N(amine) distances are unexceptional and similar to those observed for **1**. The geometry at the Re–NNR unit is consistent with the description as a metal–diazenido moiety. The Re–O(1) distance of 2.06 (2) Å suggests that the diazenido unit exerts no significant trans influence upon the oxygen-bonded sulfinato ligand, an observation in agreement with previous discussions.[21] The S(2)–O(1) and S(2)–O(2) distances, 1.51 (2) and 1.53 (3) Å are similar to those observed for sodium hydroxymethanesulfinate dihydrate,[24] 2-guanidoethanesulfinic acid,[25] and other examples of oxygen-bonded sulfinato groups.[10] The valence angles about S(2) are consistent with a trigonal-pyramidal geometry. In contrast, the second sulfinato-unit coordinates through the sulfur S(1) with a Re–S(1) distance at 2.39 Å. The S(1)–O(3) and S(1)–O(4) distances of 1.46 (2) and 1.45 (2) Å are significantly shorter than the distances observed for S(2)–O(1) and S(2)–O(2). Analogous trends have been observed for other S-bonded sulfinato ligands[10] and for coordinated SO_3^{2-}.[26] On the basis of arguments by Kierkegaard[27] and Cruikshank,[28] bonding of the SO_3^{2-} or RSO_2^- sulfur lone pair will serve to strengthen and shorten the S–O bond by increasing the π-bond order. The opening of the O(3)–S(1)–O(4) angle of 113.0 (11)°, as compared to 106.1 (12)° for O(1)–S(2)–O(2), is consistent with these arguments. The most unusual feature of the structure is the presence of both S-bonded and O-bonded sulfinato residues.

The tetradentate ligand forms three chelate rings with the metal. The C–S(1)–Re–N(3)–C ring exhibits an asymmetric skew conformation, while the other five-membered ring C–N(3)–Re–N(4)–C is in the symmetric skew form with both methyl groups on the same side of the N(3)–Re–N(4) plane. The six-membered ring C–S(2)–O(1)–Re–N(4)–C adopts a skew conformation.

Electrochemical Studies. The complexes $[Re(SXXS)(PPh_3)(N_2R)]$ were examined by cyclic voltammetry at a platinum-wire electrode in acetonitrile containing 10^{-1} M $(n\text{-}Bu_4N)PF_6$. The overall electrochemical characteristics are similar for all members of this class of compounds, as illustrated by the data summarized in Table VIII. The primary oxidation process is electrochemically reversible for each complex at scan rates greater than 0.5 V s^{-1}. The second anodic wave is irreversible even at scan rates of 20 V s^{-1}, indicating that the dication undergoes rapid chemical reaction to unidentified products. These oxidation processes are summarized by the following reaction scheme:

$$[Re(SXXS)(PPh_3)(N_2R)] \underset{+1e^-}{\overset{-1e^-}{\rightleftharpoons}} [Re(SXXS)(PPH_3)(N_2R)]^+ \xrightarrow{-1e^-} [Re(SXXS)(PPh_3)(N_2R)]^{2+} \text{ (unstable)}$$

Although the monopositive cation is stable on the cyclic voltammetric time scale, attempts to prepare the species by controlled-potential electrolysis resulted in the discharge of the characteristic orange-brown color of the neutral complex and the formation of an intractable precipitate. Similarly, chemical oxidation in various solvents with $AgPF_6$ or I_2 failed to isolate the monopositive cation.

The reduction of the neutral rhenium–diazenido complexes occurs only at highly negative potentials, ca. −1.30 to −1.90 V. This shows that the lowest unoccupied molecular orbital (LUMO) is ca. 40–55 kcal higher in energy than the highest occupied molecular orbital (HOMO) of the closed-shell species. Complexes possessing the linear metal–diazenido functionality are generally electrochemically inactive toward reduction or exhibit large negative reduction potentials.[30–32] The tendency for multiple M–N bond formation to give closed-shell 18-electron complexes with no low-lying unoccupied orbitals is strong, and the disruption of the dπ–pπ M–N bonding is not a ready process.

If we assume that changes in solvation energy differences for the series of complexes of the type $[Re(SXXS)(PPh_3)(N_2R)]$ are negligible, then the potential of the reversible oxidation may be taken as a measure of the energy of the HOMO of each complex. The primary oxidation potentials show the expected trend: the more electron withdrawing the substituent R, the more positive is the oxidation potential, or the lower the energy of the HOMO.

Controlled-potential reduction at potentials of ca. −2.00 V show linear current against charge passed plots with the consumption of 3e/mol of complex. The reduction product (R) is not stable and reacts rapidly with protons from residual water in the solvent. This product also reacts rapidly with HCl–diethyl ether and upon base extraction and analysis reveals the presence of the free hydrazine $H_2NNHCOPh$ in 40% yield. The electroreduction presumably activates the $[ReN_2R]$ group toward protic attack:

$$[Re(SXXS)(PPh_3)(NNR)] \xrightarrow{+3e^-} (R) \xrightarrow{3H^+} H_2NNHR$$

The data in Table VIII also show that the lowest energy transition in the UV–visible spectra of the (aryldiazenido)rhenium complexes is a charge-transfer band with ϵ = 4000- to 8000 L mol^{-1} cm^{-1}. This is an intramolecular process, and the transition wavelength is independent of solvent. This band appears to be

---

(24) Truter, M. R. *J. Chem. Soc.* **1962**, 3400.

(25) Berthou, J.; Laurent, A.; Rinsky, A. *C. R. Seances Acad. Sci., Ser. C* **1972**, *274*, 157.

(26) Kierkegaard, P.; Larsson, L. O. *Acta Chem. Scand.* **1969**, *13*, 2253. Baggio, S.; Becka, J. W. *Acta Crystallogr., Sect. B: Struct. Crystallogr. Cryst. Chem.* **1969**, *25*, 946.

(27) Kierkegaard, P.; Larsson, L. O.; Nyberg, B. *Acta Chem. Scand.* **1972**, *26*, 218.

(28) Cruikshank, D. W. J. *J. Chem. Soc.* **1961**, 5486.

(29) Chatt, J.; Rowe, G. A. *J. Chem. Soc. A* **1962**, 4019.

(30) Butler, G.; Chatt, J.; Leigh, G. J. *J. Chem. Soc., Dalton Trans.* **1979**, 113.

(31) Bishop, M. W.; Butler, G.; Chatt, J.; *J. Chem. Soc., Dalton Trans.* **1979**, 1834.

(32) Crichton, B. A. L.; Dilworth, J. R.; Pickett, C. J.; Chatt, J. *J. Chem. Soc., Dalton Trans.* **1981**, 419.

(33) The periodic group notation in parenthesis is in accord with recent actions by IUPAC and ACS nomenclature committees. A and B notation is eliminated because of wide confusion. Groups IA and IIA become groups 1 and 2. The d-transition elements comprise groups 3 through 12, and the p-block elements comprise groups 13 through 18. (Note that the former Roman number designation is preserved in the last digit of the new numbering: e.g., III → 3 and 13.)

Table VIII. Electrochemical and Electronic Parameters of Rhenium–Organodiazenido Complexes[a]

complex	$E_{1/2}$ or E_p,[a] V	$E_p^f - E_p^r$, mV	(i_p^f/i_p^r)	$i_p/Cv^{1/2}$,[d] mA $s^{1/2}$ $mV^{-1/2}$ M^{-1}	e/Re[e]	λ, nm	$10^{-3}\epsilon$, L mol^{-1} cm^{-1}
1	+1.005	*c*	*c*	8.4	1.0	412	8.0
	+0.493	72	1.1	8.1	1.0		
	−1.410	*c*	*c*	14.3	3.1		
2a	+1.091	*c*	*c*	8.3	1.0	415	5.0
	+0.356	71	1.0	7.9	1.0		
	−1.903	*c*	*c*	15.6	3.0		
3	+1.115	*c*	*c*	8.0	1.0	406	4.2
	+0.650	70	1.1	7.9	1.0		
	−1.310	*c*	*c*	14.6	2.9		

[a] At a platinum-bed working electrode, using solutions 1.0 × 10^{-3} M in complex in 0.1 M $(Bu_4N)PF_6$ in CH_2Cl_2. All potentials are referred to the ferrocene/ferrocenium (*n*-couple). Cyclic voltammograms were obtained at a sweep rate of 200 mV s^{-1}. [b] Estimated from $E_{1/2}^{ox} = (E_p^{ox} - E_p^{red})/2 \sim E_p^{ox} - 29$ mV. The shape parameter $E_p^{ox} - E_{p/2}^{ox}$ lay within the range 60–80 mV for all complexes. [c] No reverse wave observed. [d] The current function for the ferrocene/ferrocenium couple at the same electrode is 8.5 mA $s^{1/2}$ $mV^{-1/2}$ M^{-1}. [e] The value of e/Re was determined by controlled-potential electrolysis at a potential 0.2 V from the process of interest.

Table IX. Summary of Crystal Data and Experimental Details for the Structures of $[Re\{SCH_2CH_2N(CH_3)CH_2CH_2N(CH_3)CH_2CH_2S\}(N_2COC_6H_4Cl)(PPh_3)]\cdot CH_3OH$ (**1**), $[Re(SCH_2CH_2SCH_2CH_2CH_2SCH_2CH_2S)(NNCOC_6H_5)(PPh_3)]$ (**2**), $[Re(SCH_2CH_2SCH_2CH_2CH_2SCH_2CH_2S)(NNCO_2Me)(PPh_3)]\cdot CH_2Cl_2$ (**3**), and $[Re\{O_2SCH_2CH_2N(CH_3)CH_2CH_2N(CH_3)CH_2CH_2SO_2\}(NNC_6H_4\text{-}o\text{-}Cl)(PPh_3)]$ (**5**)

	1	2	3	5
(A) Crystal Parameters at 23 °C[a]				
a, Å	8.683 (2)	11.804 (3)	8.570 (2)	9.060 (3)
b, Å	18.278 (4)	12.529 (3)	10.720 (2)	10.499 (3)
c, Å	24.691 (4)	21.448 (4)	35.618 (6)	19.058 (4)
α, Å deg	90.00 (1)	90.00	90.00 (1)	78.18 (1)
β, deg	97.95 (1)	89.39 (1)	90.14 (1)	84.85 (1)
γ, deg	97.00 (1)	90.00	90.00 (1)	76.34 (1)
V, $Å^3$	3881.2 (8)	3171.8 (9)	3272.3 (11)	1722.5 (10)
space group[g]	$P2_1/n$	$P2_1/n$	$P2_1/n$	$P\bar{1}$
Z	4	4	4	2
D_{calcd}, g/cm^3	1.41	1.69	1.54	1.65
(B) Measurement of Intensity Data				
cryst dimens, mm	0.20 × 0.18 × 0.24	0.15 × 0.29 × 0.20	0.21 × 0.25 × 0.11	0.14 × 0.16 × 0.17
instrument	Nicolet R3m			
radiation	Mo Kα (λ = 0.71073 Å)			
scan mode	coupled θ(cryst)–2θ(counter)			
scan rate, deg/min	7–30			
scan range, deg	2 < 2θ ≤ 45			
scan length, deg	from 2θ($Kα_1$) − 1.0 to 2θ($Kα_2$) + 1.0			
bkgd meas	stationary cryst, stationary counter, at the beginning and end of each 2θ scan, each for the time taken for the scan			
stds	3 collcd every 197			
no. of reflcns collcd	4563	6321	6425	4542
no. of indep reflcns used in solution: $I_o \geq 3\sigma(I_o)$	2469	2981	3172	3395
(C) Reduction of Intensity Data and Summary of Structure Solution and Refinement[b]				
abs coeff, cm^{-1}	35.49	73.15	43.26	40.88
abs cor	based on ψ scans for 5 reflections with χ angles near 90° or 270°			
T_{max}/T_{min}	1.14	1.21	1.09	1.10
structure solution	Patterson synthesis yielded the Re positions; all remaining non-hydrogen atoms located via standard Fourier techniques			
atom scattering factors[c]	neutral atomic scattering factors used throughout the analysis			
anomalous dispersion[d]	applied to all non-hydrogen atoms			
final discrepancy factors[e]	*R* = 0.055 R_w = 0.060	*R* = 0.068 R_w = 0.071	*R* = 0.059 R_w = 0.061	*R* = 0.077 R_w = 0.082
goodness of fit[f]	1.052	1.683	1.420	1.689

[a] From a least-squares fitting of the setting angle of 25 reflections. [b] All calculations were performed on a Data General Nova 3 computer with 32K of 16-bit words using local versions of the Nicolet SHELXTL interactive crystallographic software package as described in: Sheldrick, G. M. *Nicolet SHELXTL Operations Manual*: Nicolet XRD Corp.: Cupertino, CA, 1979. Data corrected for background, attenuators, Lorentz, and polarization effects in the usual fashion. [c] *International Tables for X-ray Crystallography*; Ber Kynoch: Birmingham, England, 1974; Vol. IV. [d] *International Tables for X-ray Crystallography*; Ber Kynoch: Birmingham, England, 1974; Vol. III. [e] $R = \sum[|F_o| - |F_c|/\sum|F_o|]$, $R_w = [\sum w(|F_o| - |F_c|)^2/\sum wF_o^2]^{1/2}$, $w = 1/\delta^2(F_o) + g^*(F_o)$, and $g = 0.005$. [f] GOF = $[\sum w(|F_o| - |F_c|)^2/(NO - NV)]^{1/2}$ where NO is the number of observations and NV is the number of variables. [g] Nonstandard settings are reported for compounds **2** and **5**. The cells with acute angles were used for convenience during data collection and inadvertently retained throughout the structure analysis, including archiving.

associated with the [Re–N–N–R] chromophore, as previously discussed. The wavelength of this transition is not sensitive to the diazenido substituent R for the complexes, which exhibits peak absorptions at ca. 410 nm. Either both orbitals associated with the charge-transfer band are insensitive to the nature of R or both donor and acceptor orbitals are shifted in energy to a similar extent as R is varied. Since the former argument would preclude the HOMO as the donor orbital, this rationalization appears unlikely.

Conclusions. The structures of the rhenium–diazenido species $[Re\{SCH_2CH_2X(CH_2)_nXCH_2CH_2S\}(NNR)(PPh_3)]$, R = –COPh or $-CO_2R$, are unusual with respect to the arrangement of thiolate donors. The cis conformation of the thiolate donors is exceptional as is the disposition of a thiolate donor trans to the strongly π-bonding diazenido ligand. The geometry may reflect a substitution pattern imposed by the synthetic precursors, the green hydrazido(3−)-*O,N′*-chelates, $[ReCl_2(PPh_3)_2(NNR)]$, whose substitution reactions occur via chelate ring opening to give an organodiazenido linkage and insertion of a neutral two-electrons donor into the now vacant coordination site. In the absence of further reorganization of the coordination sphere, the thiolate donors are constrained to adopt the cis configuration. A *pseudocis* orientation of thiolate donors has been observed previously only for ligands with exceptional steric requirements.

The chemistry of the complexes is also dramatically influenced by the substituent R of the organodiazenido functionality, −NNR. Thus, whereas for R = −COPh or $-CO_2Me$, the complexes $[Re\{SCH_2CH_2X(CH_2)_nXCH_2CH_2S\}(PPh_3)(N_2R)]$ are stable toward oxidation, for R = $-C_6H_4X$, the complexes are found to undergo facile oxidation to the sulfinato-coordinated species $[Re\{O_2SCH_2CH_2N(CH_3)CH_2CH_2N(CH_3)CH_2CH_2SO_2\}(PPh_3)(NNR)]$. Complex **5** represents the first example of a species presenting both O-bonded and S-bonded sulfinato ligands. It is tempting to speculate that the location of the O-bonded sulfinato donor trans to the diazenido linkage reflects the strong trans influence of this ligand upon the sulfur donor of the reduced precursor, allowing insertion of oxygen into the metal–sulfur bond in the oxidation step.

Experimental Section

Materials and Methods. All preparative reactions were performed in freshly distilled, dry solvents, and unless otherwise noted no special precautions to eliminate atmospheric oxygen were taken. Reagent grade solvents were used throughout. $[ReOCl_3(PPh_3)_2]$ was prepared by the literature method.[29] All other reagents were obtained from standard commercial sources and used without further purification.

The following instruments were used in this work: IR, Perkin-Elmer 283B infrared spectrophotometer; UV–visible, Varian DMSO 90 UV–visible spectrophotometer; X-ray crystallography, Nicolet R3m diffractometer; electrochemistry, BAS 100 electroanalytical system.

All compounds were isolated as crystalline solids. Microanalytical data were obtained by MicAnal, Tucson, AZ.

Synthesis of $[ReCl_2(PPh_3)_2(NNCOC_6H_4Cl)]$ (1a). Oxotrichlorobis(triphenylphosphine)rhenium (2.0 g), 4-chlorobenzoic acid hydrazide (2.3 g), and triphenylphosphine (2.0 g) were heated under reflux with stirring in 15 mL of 1 M HCl in 25 mL of ethanol and 50 mL of dichloromethane for 30 min, after which 50 mL of heptane was added to form a bright green precipitate. Yield: 65%.

Synthesis of $[Re(PPh_3)(NNCOC_6H_4Cl)(SCH_2CH_2N(CH_3)CH_2CH_2N(CH_3)CH_2CH_2S)]$ (1). [*N*-(4-Chlorobenzoyl)hydrazido-*N,O*]dichlorobis(triphenylphosphine)rhenium (V) (**1a**) (0.80 g) in 150 mL of benzene was added to 0.90 g of *N,N′*-dimethyl-*N,N′*-bis(2-mercaptoethyl)ethylenediamine and 0.75 mL diisopropylethylamine in 50 mL of benzene. The mixture was warmed gently with stirring for 1 h. A brown precipitate began to form as the color darkened. The solution was then filtered and the precipitate discarded. The benzene was removed from the filtrate by rotary evaporation. The resulting red-brown oil was dissolved in dichloromethane and layered with methanol–diethyl ether. Red-brown crystals formed gradually. Yield: 40%. Anal. Calcd for $[Re(PPh_3)(NNCOC_6H_4Cl)\{SCH_2CH_2N(CH_3)CH_2CH_2N(CH_3)CH_2CH_2S\}]$: C, 47.8; H, 4.8; N, 6.5;, S, 7.5. Found: C, 47.9; H, 4.8; N, 6.3; S, 7.3. Electronic spectrum, λ (ϵ, L mol^{-1} cm^{-1}): 412 (8.0 × 10^3), 345 (1.25 × 10^4), 238 nm (2.38 × 10^4).

Synthesis of $[Re(PPh_3)(NNCOC_6H_5)(SCH_2CH_2SCH_2CH_2CH_2SCH_2CH_2S)]$ (2). (*N*-Benzoylhydrazido-*N,O*)dichlorobis(triphenylphosphine)rhenium (**2a**) (0.4 g) in 80 mL of benzene was added to 1,4,8,11-tetrathiaundecane (0.1 g) and diisopropylethylamine (0.3 mL) in 30 mL of benzene. The resulting solution was stirred at room temperature overnight. The red-brown solution was filtered and any insoluble material discarded. The benzene was removed by rotary evaporation and the resulting red oil dissolved in dichloromethane and layered with methanol–diethyl ether. Dark red crystals formed when the mixture was allowed to sit at room temperature. Yield: 60%. Anal. Calcd for $[Re(PPh_3)(NNCOPh)(SCH_2CH_2SCH_2CH_2CH_2SCH_2CH_2S)]$: C, 47.6; H, 4.2; N, 3.5; S, 15.8. Found: C, 47.6; H, 4.0; N, 3.5; S, 15.6. Electronic spectrum, λ (ϵ, L mol^{-1} cm^{-1}): 415 (5.0 × 10^3), 355 (8.1 × 10^3), 320 (1.3 × 10^4)8 238 nm (1.5 × 10^4).

Synthesis of $[ReCl_2(PPh_3)_2\{(CH_3)_2NCHO\}(NNCOOCH_3)]$ (3a). Oxotrichlorobis(triphenylphosphine)rhenium (2.0 g), triphenylphosphine (2.0 g), and methylhydrazinecarboxylate (1.33 g) in 150 mL of ethanol were added to 50 mL of dimethylformamide, 20 mL of dichloromethane, and 20 mL of 1 M HCl in ethanol and refluxed with stirring for 90 min. Ethanol and dichloromethane were removed by rotary evaporation, leaving a red-purple precipitate forming in the remaining dimethylformamide. The precipitate was washed with methanol. Yield: 45%. Anal. Calcd for $[ReCl_2(PPh_3)_2(DMF)(NNCOOCH_3)]$: C, 52.2; H, 4.3; N, 4.5; Found: C, 52.3; H, 4.3; N, 4.4.

Synthesis of $[Re(PPh_3)(NNCOOCH_3)(SCH_2CH_2SCH_2CH_2SCH_2CH_2S)]$ (3). [(Carboxymethyl)azo]dichlorobis(triphenylphosphine)(dimethylformamide)rhenium (**3a**), (1.28 g), 1,4,8,11-tetrathiaundecane (0.70 g), and diisopropylethylamine (1.5 mL) in 150 mL of benzene were stirred overnight at room temperature. The resulting solution was filtered and the precipitate discarded. Benzene was removed from the filtrate by rotary evaporation giving a red-brown oil, which was dissolved in dichloromethane and layered with methanol–diethyl ether. Red crystals formed gradually at room temperature. Yield: 60%. Anal. Calcd for $[Re(PPh_3)(NNCOOCH_3)(SCH_2CH_2S(CH_2)_3SCH_2CH_2S)]$: C, 40.2; H, 4.1; N, 3.4. Found: C, 40.0; H, 4.1; N, 3.4. Electronic spectrum, λ (ϵ, L mol^{-1} cm^{-1}: 406 (4.2 × 10^3), 350 (sh), 320 (5.5 × 10^3), 235 (7 (1.22 × 10^4).

Synthesis of $[ReCl_2(PPh_3)_2(NH_3)(NNC_6H_4Cl)]$ (4a). Oxotrichlorobis(triphenylphosphine)rhenium (2.0 g), (2-chlorophenyl)hydrazine hydrochloride (2.0 g), and triphenylphosphine (2.0g) were heated under reflux with stirring in 100 mL of benzene and 100 mL of ethanol for 45 min. An orange precipitate formed from the red-brown solution and was separated by filtration. Solvents were removed from the filtrate by rotary evaporation. Upon trituration of the resulting red-brown oil with anhydrous diethylether, a tan material precipitated which was isolated by filtration and washed with anhydrous diethyl ether. The tan precipitate was next washed with dichloromethane, which solubilized the ammonia complex, giving a dark red solution. Crystals formed by slow evaporation of the dichloromethane solution under air. Yield: 15%.

Synthesis of $[Re(PPh_3)(NNC_6H_4Cl)\{SO_2CH_2CH_2N(CH_3)CH_2CH_2N(CH_3)CH_2CH_2SO_2\}]$ (5). Dichloro[(2-chorophenyl)diazenido](ammine)bis(triphenylphosphine)rhenium (0.7 g) (**4a**), *N,N′*-dimethyl-*N*,-*N′*-bis(2-mercaptoethyl)ethylenediamine (1.5 g), and diisopropylethylamine (1.5 mL) in 150 mL of benzene were gently warmed with stirring overnight. The resulting red solution was filtered and benzene removed by rotary evaporation. The red-brown oily residue (**4**) was eluted from a silica column with tetrahydrofuran–ethanol (50:50). The red component eluted rapidly, leaving a brown material on the column. Recrystallization from tetrahydrofuran–*n*-pentane gave cherry red crystals in 15% yield.

X-ray Crystallography. The details of the crystal data, data collection methods, and refinement procedures are given in Table IX. Full details of the crystallographic methodologies may be found in ref 19.

Acknowledgment. We gratefully acknowledge a gift of $NaReO_4$ from Dr. Barry Haymore of Monsanto Corp., St. Louis, MO.

Supplementary Material Available: Tables of bond lengths and angles, anisotropic temperature factors, and calculated hydrogen atom positions (24 pages); tables of observed and calculated structure factors (141 pages). Ordering information is given on any current masthead page.